Combined Virtual/Experimental Multicomponent Solid Forms Screening of Sildenafil: New Salts, Cocrystals and Hybrid Salt-Cocrystals

Rafael Barbas,[†] *Mercè Font-Bardia,*[§] *Anant Paradkar,*[‖] *Christopher A. Hunter*[‡] *and Rafel Prohens**[†]

[†] Unitat de Polimorfisme i Calorimetria, Centres Científics i Tecnològics, Universitat de Barcelona, Baldiri Reixac 10, 08028 Barcelona, Spain

[§] Unitat de Difracció de Raigs X, Centres Científics i Tecnològics, Universitat de Barcelona.

[‖] Centre for Pharmaceutical Engineering Science. School of Pharmacy, University of Bradford
[‡] Department of Chemistry, University of Cambridge

RECEIVED DATE (to be automatically inserted after your manuscript is accepted if required according to the journal that you are submitting your paper to)

*To whom correspondence should be addressed. E.mail: rafel@ccit.ub.edu

ABSTRACT: New multicomponent solid forms of Sildenafil have been discovered by means of a combined virtual/experimental cocrystal screening. Coformer selection of candidates was conducted based on an *in silico* screening method from a database of more than 2000 organic compounds and the intensive experimental screen produced 23 new solid forms. Since the 12 coformers chosen have a combination of phenol and carboxylic acid groups a variety of cocrystals, salts and hybrid salt/cocrystals were discovered and characterized.

INTRODUCTION

Cocrystals of Active Pharmaceutical Ingredients (APIs) have received a massive attention over the last decade because they offer many opportunities to improve physicochemical properties of drugs.[1,2] Indeed, solubility is one of the most important properties for a drug compound since it has a direct impact on the bioavailability and the cocrystal approach is a versatile toolbox to tune this and another important property[3,4] such as stability[5] because the high number of available potential coformers.

On february 2018, FDA released a final guidance titled "Regulatory Classification of Pharmaceutical Co-Crystals Guidance for Industry",[6] providing applicants planning to submit new drug applications with information on the regulatory classification of pharmaceutical cocrystals, with a similar treatment to that of a new polymorph, and not as a new API. FDA asks the applicants to provide evidences to demonstrate that "both the API and coformers are present in the unit cell" and "the component API and coformer co-exist in the cocrystal which interact nonionically". The FDA guidance suggests the applicant to consider the difference of ΔpKa between the API and the coformer or to provide evidences that proton transfer has not ocurred in the lattice by means of spectroscopic tools or other orthogonal approaches. Thus, from a regulatory point of view it is very important to assess the proton transfer in a multicomponent drug solid form. In this sense, hybrid salt/cocrystals are located in the middle of the salt/cocrystal continuum and can constitute a particular case to be considered during the formulation of a new solid form.[7]

Sildenafil, the active principle of Viagra, is the first oral drug used for the medical treatment of erectile dysfunction in elderly patients and it was initially used as an antihypertensive drug[8, 9] but due to its poor aqueous solubility and low bioavailability it is generally formulated as sildenafil citrate.[10] This solid form still exhibits moderate bioavailability and this is the reason why some efforts have been conducted to discover new salts and cocrystals with enhanced physicochemical properties. In this sense, a sildenafil/acetylsalicylic cocrystal exhibiting enhanced intrinsic dissolution rate compared to sildenafil

citrate has been reported. Moreover, pharmacokinetics of salts and cocrystals of sildenafil with dicarboxylic acids has been studied and the glutarate salt was revealed to be a good candidate for alternative formulation of the citrate salt.[11] The crystal structures of sildenafil base, sildenafil citrate monohydrate and sildenafil saccharinate have been published in the literature[12] and some of us have described a new polymorph of Sildenafil free base and new solvates.[13,14] With the aim to discover new multicomponent forms and extend the solid state knowledge of this important API we have conducted a combined virtual/experimental salt/cocrystal screening by using a broad set of thermodynamic and kinetic experimental conditions. 23 new solid forms of sildenafil, including salts, cocrystals and hybrid salt/cocrystals, have been discovered and some of their crystal structures solved.

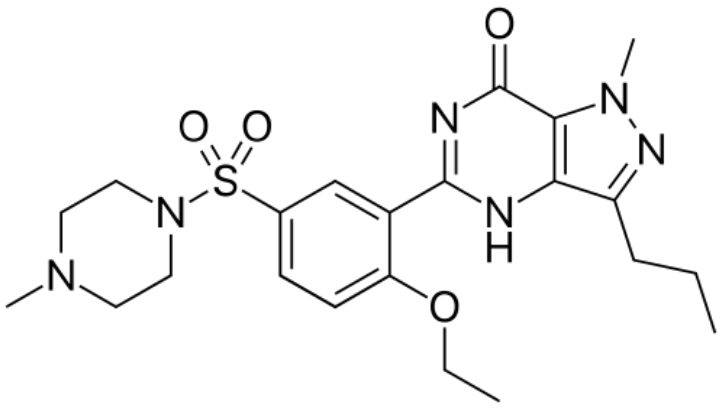

Figure 1. Molecular structure of sildenafil.

2 MATERIALS AND METHODS

2.1. Materials

Sildenafil (SIL) used in this study was of reagent grade and used as received from Polpharma (form I). The coformers quercetin (QUE), methyl gallate (MEG), tartaric acid (TAR), 3-hydroxybenzoic acid (3-HBA), 4-hydroxybenzoic acid (4-HBA), resorcinol (RES), 3,4-dihydroxybenzoic acid(3,4-DHBA) and caffeic acid (CAF) where purchased from Sigma-Aldrich.

2.2 Methods

2.2.1 Virtual Cocrystal Screening: For each compound, the molecule was drawn in an extended conformation and energy minimised using the molecular mechanics methods implemented in TorchLite.[15] Gaussian 09 was used to optimise the geometry and calculate the MEPS on the 0.002 Bohr $Å^{-3}$ electron density isosurface using DFT and a B3LYP/6-31G* basis set.[16] The MEPS was converted into SSIPs using in-house software.[17]

2.2.2 Cocrystal Screening: Screening through liquid assisted grinding experiments (LAG) was conducted by grinding 20-35 mg of a 1:1 mixture of SIL and each coformer together with one drop of different solvents using a Retsch MM 2000 grinding mill. The samples were placed in 2 mL volume stainless steel jars, along with two stainless tungsten grinding balls of 3 mm diameter. Grinding was performed for 15-30 minutes, with a frequency of the mill of 30 Hz. Finally, the samples were collected immediately without prior drying for PXRD analysis. The formation of a new solid form was determined by comparing PXRD patterns of starting materials and products from cocrystal screening LAG experiments. Screening through reaction crystallization (RC) was conducted by preparing a saturated solution of the most soluble component (SIL or coformer) in different solvents in a sealed vial under stirring. A small quantity of the less soluble component was added until it did not dissolve anymore. The suspension was stirred at different times and the resulting solids were filtered and analyzed by PXRD. Screening through solvent mediated transformations (SMT) were conducted by preparing suspensions of SIL and coformer in different molar ratios (40-1200 mg of the final mixture) in selected solvents. The sealed vials were stirred for different times and the resulting solids were filtered and analyzed by PXRD.

2.2.3 Solution Crystallization: Solutions of SIL:coformer in a 1:1 molar ratio (10-20 mg of the final mixture) were prepared in different solvents and heated up in a heating stainless steel block. The heater was switched off and the solutions were allowed to slowly cool down to room temperature inside the heating block. The samples which did not crystallize were tightly sealed and kept at 25 ºC until precipitation was observed.

2.2.4 Synthesis of the different crystal forms of Sildenafil

Details of synthesis and characterization of each form can be found at ESI section. Stoichiometry has been assessed based on NMR and TGA measurements when crystal structure is not available. In those cases where crystal structure has not been solved the definition of the form as a salt or a cocrystal has been done based on the probability of proton transfer determined with equation 3.

2.2.4.1 Quercetin cocrystal (1:1) isopropanol solvate (SIL-QUE) I. It was obtained by reaction crystallization in IPA, (m.p. 140 ºC). Its PXRD diagram has been indexed.

2.2.4.2 Quercetin cocrystal (1:1) tetrahydrofuran solvate (SIL-QUE) II. It was obtained by solvent mediated transformation in THF, (m.p. 143 ºC). Its PXRD diagram has been indexed.

2.2.4.3 3,4-dihydroxybenzoic acid salt (1:1) isopropanol solvate (SIL-3,4-DHBA) I. It was obtained by solvent mediated transformation in IPA, (m.p 105 ºC). Its PXRD diagram has been indexed.

2.2.4.4 3,4-Dihydroxybenzoic acid acid hybrid salt-cocrystal (1:2) acetonitrile solvate (SIL-3,4-DHBA) II. It was obtained by slow evaporation in ACN at 25 ºC, (3 days).

2.2.4.5 3,4-Dihydroxybenzoic acid hybrid salt-cocrystal (1:2) acetonitrile solvate (SIL-3,4-DHBA) III. It was obtained by solvent mediated transformation in acetonitrile, (m.p 99 ºC). Its PXRD diagram has been indexed.

2.2.4.6 3,4-Dihydroxybenzoic acid hybrid salt-cocrystal (2:3) dihydrate (SIL-3,4-DHBA) IV. It was obtained by slow evaporation in IPA at 25 ºC, (3 days).

2.2.4.7 Resorcinol cocrystal (1:1) (SIL-RES) I. It was obtained by solvent mediated transformation in IPA, (m.p 117 ºC). Its PXRD diagram has been indexed.

2.2.4.8 Resorcinol cocrystal (1:2) (SIL-RES) II. It was obtained by solvent mediated transformation in xylene, (m.p 152 ºC). Its PXRD diagram has been indexed.

2.2.4.9 Tartaric acid salt (1:1) (SIL-TAR) I. It was obtained by liquid assisted grinding in IPA. Its PXRD diagram has been indexed.

2.2.4.10 Tartaric acid salt (2:1) (SIL-TAR) II. It was obtained by solvent mediated transformation in THF, (m.p 152 ºC). Its PXRD diagram has been indexed.

2.2.4.11 Tartaric acid salt (1:1) isopropanol solvate (SIL-TAR) III. It was obtained by solvent mediated transformation in IPA, (m.p 229 ºC). Its PXRD diagram has been indexed.

2.2.4.12 Tartaric acid salt (2:1) isopropanol solvate (SIL-TAR) IV. It was obtained by slow evaporation in IPA/THF at 25 ºC, (3 days).

2.2.4.13 Caffeic acid salt (2:3) monohydrate (SIL-CAF) I. It was obtained by solvent mediated transformation in ACN, (m.p. 165 ºC). Its PXRD diagram has been indexed.

2.2.4.14 Caffeic acid salt (2:3) (SIL-CAF) II. It was obtained by heating SIL-CAF I at 100 ºC under N_2 atmosphere, (m.p. 164 ºC).

2.2.4.15 Methyl gallate cocrystal (1:1) (SIL-MEG). It was obtained by reaction crystallization in ACN, (m.p. 135 ºC). Its PXRD diagram has been indexed.

2.2.4.16 3-Hydroxybenzoic acid salt (1:1) acetonitrile solvate (SIL-3-HBA) I. It was obtained by reaction crystallization in ACN, (m.p. 161 ºC).

2.2.4.17 3-Hydroxybenzoic acid salt (1:1) tetrahydrofuran solvate sesquihydrate (SIL-3-HBA) II. It was obtained by slow evaporation in THF at 25 ºC, (53 days).

2.2.4.18 3-Hydroxybenzoic acid salt (1:1) (SIL-3-HBA) III. It was obtained by solvent mediated transformation in IPA, (m.p. 156 ºC).

2.2.4.19 3-Hydroxybenzoic acid hybrid salt-cocrystal (2:3) dihydrate (SIL-3-HBA) IV. It was obtained by slow evaporation in ACN at 25 ºC, (51 days).

2.2.4.20 4-Hydroxybenzoic acid salt (1:1) (SIL-4-HBA) I. It was obtained by liquid assisted grinding in ACN.

2.2.4.21 4-Hydroxybenzoic acid salt (1:1) (SIL-4-HBA) II hemiisopropanol solvate. It was obtained by reaction crystallization in IPA, (m. p. 136 ºC).

2.2.4.22 4-Hydroxybenzoic acid salt (1:1) (SIL-4-HBA) III. It was obtained by reaction crystallization in ACN, (m. p. 107 ºC).

2.2.4.23 4-Hydroxybenzoic acid salt (1:1) tetrahydrofuran solvate (SIL-4-HBA) IV. It was obtained by solvent mediated trandformation in THF, (m.p. 130ºC).

2.2.5 X-ray crystallographic analysis.

Single crystal X-ray diffraction intensity data of the different crystal forms of Sildenafil were collected using a D8 Venture system equipped with a multilayer monochromator and a Mo microfocus (λ =

0.71073 Å). Frames were integrated with the Bruker SAINT software package using a SAINT algorithm. Data were corrected for absorption effects using the multi-scan method (SADABS).[18] The structures were solved and refined using the Bruker SHELXTL Software Package, a computer program for automatic solution of crystal structures and refined by full-matrix least-squares method with ShelXle Version 4.8.0, a Qt graphical user interface for SHELXL computer program.[19]

Powder X-ray diffraction patterns were obtained on a PANalytical X'Pert PRO MPD diffractometer in transmission configuration using Cu Kα1+2 radiation (λ = 1.5406 Å) with a focusing elliptic mirror and a PIXcel detector working at a maximum detector's active length of 3.347°. Configuration of convergent beam with a focalizing mirror and a transmission geometry with flat sample sandwiched between low absorbing films measuring from 2 to 40º in 2θ, with a step size of 0.026° or from 2 to 70º in 2θ, with a step size of 0.013° with measuring times of 30 minutes to 4 hours. The powder diffractograms were indexed and the lattice parameters were refined by means of LeBail fits by means of Dicvol04,[20] and the space groups were determined from the systematic absences. A summary of crystal data and relevant refinement parameters are given in Tables 1 and 2.

Table 1. Crystal data for the different crystal forms of sildenafil

Structure	**SIL-TAR IV**	**SIL-3,4-DHBA II**	**SIL-3,4-DHBA IV**	**SIL-3-HBA II**	**SIL-3-HBA IV**
Empirical formula	$C_{51}H_{74}N_{12}O_{15}S_2$	$C_{40}H_{48}N_8O_{12}S$	$C_{65}H_{82}N_{12}O_{22}S_2$	$C_{31}H_{43}N_6O_9S$	$C_{65}H_{82}N_{12}O_{19}S_2$
Formula Weight	1159.34	864.92	1447.54	675.77	1399.54
Temperature (K)	293(2)	100(2)	100(2)	100(2)	100(2)
Crystal system	Triclinic	Monoclinic	Monoclinic	Monoclinic	Monoclinic
space group	P-1	P21/n	P21/c	P21/n	P21/n
a, b, c (Å)	6.3796(8) 13.4449(18) 17.620(2)	11.6418(8) 15.3849(13) 24.7913(19)	17.6070(17) 8.6938(8) 24.942(2)	17.7205(18) 8.2574(7) 22.991(2)	17.5329(10) 8.6545(4) 22.9653(13)
α, β, γ (°)	108.607(5) 98.363(6) 92.814(6)	90 102.749(3) 90	90 117.101(5) 90	90 102.748(3) 90	90 105.591(2) 90
Volume ($Å^3$)	1409.7(3)	4330.8(6)	3398.7(5)	3281.2(5)	3356.5(3)
Z, Density (calc.) (Mg/m^3)	1, 1.366	4, 1.327	2, 1.414	4, 1.368	2, 1.385
Crystal size (mm^3)	0.344 x 0.144 x 0.044	0.358 x 0.196 x 0.074	0.324 x 0.152 x 0.112	0.129 x 0.119 x 0.109	0.336 x 0.197 x 0.086
Reflections collected / unique	53107 / 6455 [R(int)=0.1123]	66326 / 8875 [R(int)=0.0949]	69444 / 7838 [R(int)=0.0722]	18923 / 4567 [R(int)=0.082]	33777 / 5726 [R(int)=0.0482]
Data / restraints / parameters	6455 / 8 / 396	8875 / 0 / 570	7838 / 2 / 460	4567 / 6 / 454	5726 / 0 / 502
Goodness-of - fit on F^2	1.105	1.070	1.024	1.017	1.038
Final R índices [$I > 2\sigma(I)$]	R1=0.0678, wR2=0.1740	R1=0.0537, wR2=0.1151	R1=0.0476, wR2=0.1084	R1=0.0504, wR2=0.1168	R1=0.0382, wR2=0.0886
CCDC	1858573	1858576	1858577	1858574	1858575

Table 2. Comparative cell parameters data[a] from SXRD and PXRD

Crystal form		a (Å)	b (Å)	c (Å)	α (°)	β (°)	γ (°)	V (Å^3)	Z	R (%)	Space group
SIL-QUE I	PXRD	42.39(2)	14.854(4)	15.059(6)	82.41(3)	138.08(2)	120.01(2)	4992(3)	5	11.1	P-1
SIL-QUE II	PXRD	22.528(8)	13.536(4)	8.007(2)	57.95(2)	95.99(3)	95.96(2)	2054(1)	2	6.69	P-1
SIL-3,4-DHBA I	PXRD	12.765(2)	13.463(1)	12.106(2)	112.03(1)	84.0929(9)	114.28(1)	1754.7(3)	2	8.41	P-1
SIL-3,4-DHBA II	SXRD	11.6418(8)	15.3849(13)	24.7913(19)	90	102.749(3)	90	4330.8(6)	4	5.37	P21/n
SIL-3,4-DHBA III	PXRD	24.947(6)	15.718(3)	11.642(3)	90	103.96(2)	90	4430(2)	4	7.76	P21/n
SIL-3,4-DHBA IV	SXRD	17.6070(17)	8.6938(8)	24.942(2)	90	117.101(5)	90	3398.7(5)	2	4.76	P21/c
SIL-RES I	PXRD	11.266(2)	14.835(2)	14.178(2)	38.099(7)	94.79(1)	96.09(9)	1453.9(3)	2	12.0	P-1
SIL-RES II	PXRD	14.2705(4)	26.083(2)	9.9925(5)	90	108.398(3)	90	3530.0(3)	4	6.20	P21/a
SIL-TAR I	PXRD	18.07(1)	13.609(6)	7.590(4)	85.98(3)	92.33(3)	110.09(4)	1749(1)	2	7.31	P-1
SIL-TAR II	PXRD	33.57(9)	15.070(3)	11.547(3)	90	90	90	5445(2)	4	8.11	P21 21 21
SIL-TAR III	PXRD	18.313(4)	15.070(3)	6.3764(9)	63.85(1)	101.56(1)	112.86(2)	1454.5(5)	2	7.64	P-1
SIL-TAR IV	SXRD	6.3796(8)	13.4449(18)	17.620(2)	108.607(5)	98.363(6)	92.814(6)	1409.7(3)	1	6.78	P-1
SIL-CAF I	PXRD	25.845(7)	8.336(1)	20.32(6)	90	121.19(1)	90	3744(2)	2	5.76	P21/m
SIL-MEG	PXRD	12.9869(8)	13.4289(8)	13.4551(8)	53.033(3)	118.580(4)	111.246(4)	1637.1(1)	2	5.04	P-1
SIL-3-HBA II	SXRD	17.7205(18)	8.2574(7)	22.991(2)	90	102.748(3)	90	3281.2(5)	4	5.04	P21/n
SIL-3-HBA IV	SXRD	17.5329(10)	8.6545(4)	22.9653(13)	90	105.591(2)	90	3356.5(3)	2	3.82	P21/n

[a] R-Factor for SXRD and Rwp for PXRD.

2.2.6 Differential Scanning Calorimetry (DSC). Differential scanning calorimetry analysis was carried out by means of a Mettler-Toledo DSC-822e calorimeter. Experimental conditions: aluminium crucibles of 40 μL volume, atmosphere of dry nitrogen with 50 mL/min flow rate, heating rate of 10°C/min. The calorimeter was calibrated with indium of 99.99% purity (m.p.: 156.4 ºC ΔH: 28.55 J/g).

2.2.7 Thermogravimetric Analysis (TGA). Thermogravimetric analyses were performed on a Mettler-Toledo TGA-851e thermobalance. Experimental conditions: alumina crucibles of 70 μL volume, atmosphere of dry nitrogen with 50 mL/min flow rate, heating rate of 10°C/min.

2.2.8 Nuclear magnetic resonance (NMR): Proton nuclear magnetic resonance (^{1}H-NMR) spectra has been recorded on a Varian Mercury 400 (400 MHz). Chemical shifts for proton are reported in parts per million (ppm) downfield from tetramethylsilane and are referenced to residual proton in the NMR solvent (dmso-d_6: δ 2.50). Experimental conditions: delay: 1; pulse: 45º; scans: 32 or 64.

2.2.9 Dissolution Study

The dissolution measurements were carried out for pure sildenafil, salts of sildenafil with citric acid, tartaric acid and 3-HBA, a cocrystal with RES, QUE and three hybrid salt-cocrystals (HSC) of sildenafil with 3,4-DHBA. The dissolution was determined in 0.1N HCl (pH 1.2), phosphate buffer pH 6.5 and a biorelevant dissolution medium Fasted State Simulated Intestinal Fluid (FaSSIF) at 25°C. For dissolution studies 40 mg crystalline compounds were added to the dissolution medium stirred at 100 rpm over 24 hours and samples were withdrawn at 1 hour and 24 hours. The amount of SIL dissolved in 1 hour (D_{1hr}) and 24 hours (D_{24hrs}) was determined using HPLC technique. The details about dissolution medium and HPLC method are provided in SI.

3 RESULTS AND DISCUSSION

3.1 Virtual cocrystal screen

We have selected the coformers for experimental screening based on the virtual cocrystal screening methodology developed by some of us to predict the probability of cocrystal formation. This computational tool has been validated using experimental data extracted from the literature.

The difference between the energy of the cocrystal and the pure components was used to rank CCFs, and CCFs that were found to form cocrystals experimentally were significantly enriched at the top of the ranked list in most cases.[21] This approach uses Surface Site Interaction Points (SSIPs) calculated from the *ab initio* molecular electrostatic potential surface (MEPS) of the isolated molecule in the gas phase.[17,22] The interaction of a molecule with its environment is described by a discrete set of SSIPs, each represented by an interaction parameter, ε_i, which is positive for a H-bond donor site (or positive region on the MEPS) and negative for a H-bond acceptor site (or negative region on the MEPS). The energy of interaction between two SSIPs, *i* and *j*, is given by the product $\varepsilon_i\varepsilon_j$. We assume that pairwise interactions between SSIPs are optimised in a solid, and this provides a method for evaluating the interaction site pairing energy of a solid without knowledge of the crystal structure.[23] The most positive SSIP is paired with the most negative SSIP, the next most positive SSIP with the next most negative, and so on, giving a hierarchical list of interactions.[24,25] This interaction site pairing strategy provides a straightforward method for estimating the energy of a solid, *E* (equation 1). The same approach can be used to estimate the energy of a cocrystal, and the difference between the interaction site pairing energies of the cocrystal and the pure components, ΔE, can be used to estimate the probability of cocrystal formation (equation 2).

$$E = \sum e_i e_j \qquad (1)$$

$$\Delta E = -(E_{cc} - E_1 - E_2) \qquad (2)$$

where E_1, E_2 and E_{cc} are the interaction site pairing energies of the pure solids, 1 and 2, and a cocrystal respectively. Note that this definition means that ΔE is always positive, and a large value indicates a high probability of cocrystal formation.

Some of us have previously applied the method to successfully predict the formation of new cocrystals (references) and in this work we have followed this theoretical approach to guide the selection of a limited number of coformers to test experimentally. Thus, the difference between the interaction site pairing energies of the 1:1 cocrystal and the pure components of a database which contains more than 2400 organic compounds (including 860 products from the GRAS list) was calculated for each sildenafil/coformer combination using equations 1 and 2, and the coformers were ranked in order of decreasing ΔE. Finally, only 12 coformers were arbitrarily chosen among the top 100 compounds according to toxicity criteria and Table 3 shows them along with their corresponding ΔE values.

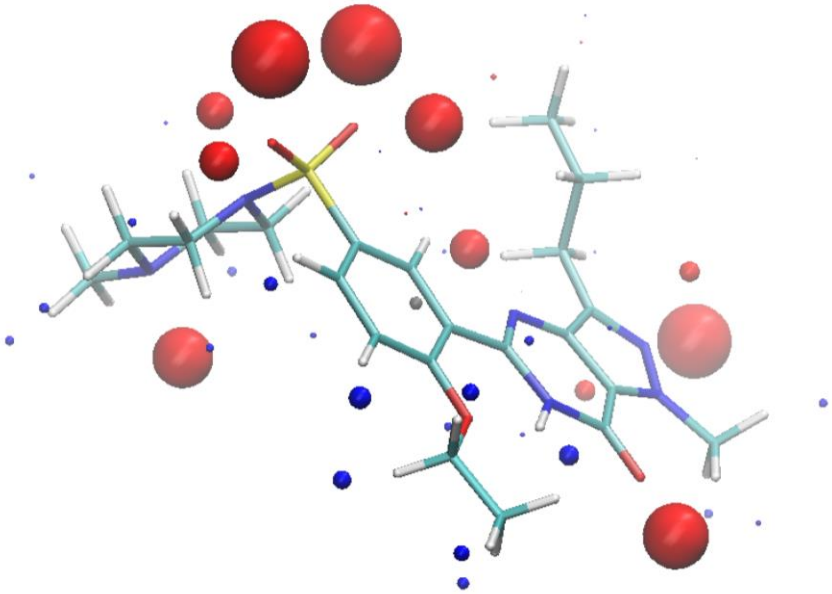

Figure 2: SSIPs calculated for sildenafil. Blue spheres correspond to H-bond donors and red spheres to H-bond acceptors.

Table 3. Coformers chosen in this study based on the difference between the interaction site pairing energies of sildenafil and the pure components, ΔE.

Coformer	ΔE / kJ mol^{-1}
Quercetin	-28,1
Resveratrol	-24,0
Phloroglucinol	-23,8
3,4-Dihydroxybenzoic acid	-21,7
Resorcinol	-19,3
Tartaric acid	-18,2
Caffeic acid	-17,8

Myo-inositol	-15,7
tert-Butylhydroquinone	-13,8
Methyl gallate	-13,5
3-Hydroxybenzoic acid	-13,1
4-Hydroxybenzoic acid	-12,9

Since sildenafil has a strong basic group, the formation of salts with strong carboxylic acids is expected. In fact, the formation of a salt or a cocrystal can be assessed based on the "rule of thumb"[26] which states that salts are formed when ΔpKa [pKa(base) – pKa(acid)] ≥ 3 and a cocrystal is expected when this value is ≤ 0, being the combinations with a value 0 ≤ [pKa(base) – pKa(acid)] ≤ 3 much less reliable and falling around a "salt-cocrystal continuum" region.[27] This uncertainty motivated the analysis and correlation by Cruz-Cabeza[28] of a big set of experimental cocrystal/salt data in order to develop a more reliable equation to predict the salt/cocrystal outcome. According to this statistical analysis, equation 3 allows to predict the probability of proton transfer around the region of ΔpKa values between -1 and 4.

$$P\ (\%) = 17\ \Delta pKa + 28 \qquad (3)$$

Sildenafil has a basic functional group (piperazine) with a pKa value of 6.78[29] and we have applied this statistical approach to the coformers with acidic groups selected from the virtual cocrystal screening to assess the probability of salt formation (Table 4).

Table 4. Cocrystal screening coformers pKa's and estimated probability of proton transfer

Coformer	Reported pKa	ΔpKa	P (%)
Quercetin	8,45[30]	-1,67	0
Resveratrol	8,49[31]	-1,71	0
Phloroglucinol	7,97[32]	-1,19	8
3,4-dihydroxybenzoic acid	4,40[32]	2,38	68
Resorcinol	9,44[32]	-2,66	0
Tartaric acid	3,03[32]	3,75	92
Caffeic acid	4,47[32]	2,31	67

Myo-inositol	12,29[31]	-5,51	0
*t*Butylhydroquinone	9,94[31]	-3,16	0
Methyl gallate	8,11[31]	-1,33	5
3-Hydroxybenzoic acid	4,08[33]	2,7	74
4-Hydroxybenzoic acid	4,57[33]	2,21	66

Coformers with acidic groups such as (3-hydroxybenzoic acid, 4-hydroxybenzoic acid, caffeic acid, 3,4-dihydroxybenzoic acid and tartaric acid) were expect to form salts. However, salt stoichiometry is an important outcome not always easy to predict because hybrid salt-cocrystal forms are also possible. In this sense, there are interesting examples in the literature with unexpected stoichiometries due to the presence of non-ionized molecules in the crystal structure such as the p-coumaric acid / quinine[34] or the *trans*-*N*,*N*′-Dibenzyldiaminocyclohexane / 2,3-dichlorophenylacetic acid[35] hybrid salt–cocrystals. Moreover, Aakeröy *etal*[36] suggested in a structural analysis of more than 80 cocrystals and salts formed between carboxylic acids and N-heterocycles that the formation of unexpected hybrid salt–cocrystals could be due to the fact that carboxylate moieties are not readily satisfied by a single hydrogen-bond donor making necessary the presence of neutral carboxylic acids in the crystal structure. We have examined the Cambridge Structural Database (Version 5.39, 2018) in order to assess the formation of hybrid salt-cocrystal forms in multicomponent crystals containing a piperazine ring (the basic group of sildenafil) and a carboxylic acid (fig 3).

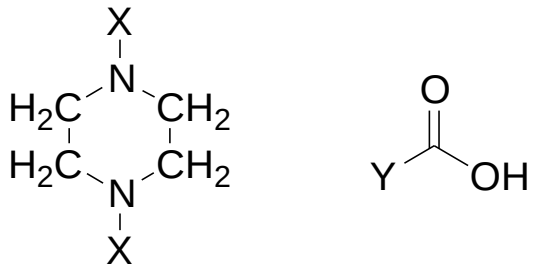

Figure 3: Fragments searched in multicomponent crystals in the CSD

A total of 247 crystal structures containing atomic coordinates were found and classified as salt, cocrystal or hybrid salt/cocrystal according to the C-O bond lenghts of the carboxylate moiety. Although 184 structures showed total proton transfer between donor and acceptor 63 of them revealed that cocrystals or mixed salt/cocrystals were formed. This encouraged us to test the carboxylic acids previously chosen in the virtual cocrystal prediction. Table 5 summarizes the results of this structural analysis.

Table 5. Classification of Multicomponent crystals with a piperazine and a carboxylic group in the CSD

Class	No. of structures	%
Salt	184	75
Cocrystal	38	15
Hybrid	25	10

3.2 Salt/Cocrystal screening

With the aim to discover new salts or cocrystals of Sildenafil an extensive multicomponent solid forms screening was conducted by using a broad set of thermodynamic and kinetic experimental conditions from a variety of 54 solvents[37] which produced 194 individual crystalline solids (see ESI for experimental and characterization details).

3.3 Crystal structures analysis

The crystal structures of 5 out of the new 23 forms of sildenafil have been solved by Single Crystal X-ray Diffraction and the following analysis shows that in all cases salts and hybrid salt/cocrystals have been formed with tartaric acid, 3-hydroxybenzoic acid and 3,4-dihydroxibenzoic acid.

3.3.1 Tartaric acid salt isopropanol hemisolvate (SIL-TAR-IV)

Tartaric acid salt isopropanol hemisolvate crystallizes with one molecule of sildenafil cation, half molecule of tartrate dianion and half disordered molecule of isopropanol in the asymmetric unit. Transfer of both protons of tartaric acid has been deduced since tartrate C-O distances are 1.18 and 1.23 Å. The dianion, which shows disorder between two conformations (in a 1:1 ratio), is encapsulated between two molecules of sildenafil establishing strong charge-assisted hydrogen bonds. Sildenafil/tartrate cages are packed with a combination of electrostatic interactions between sulphonamide moieties in a self-association fashion and weak hydrogen bonds between N-methylpyrazole rings (fig. 4 and 5). Molecular cavities are present and occupied by disordered molecules of isopropanol.

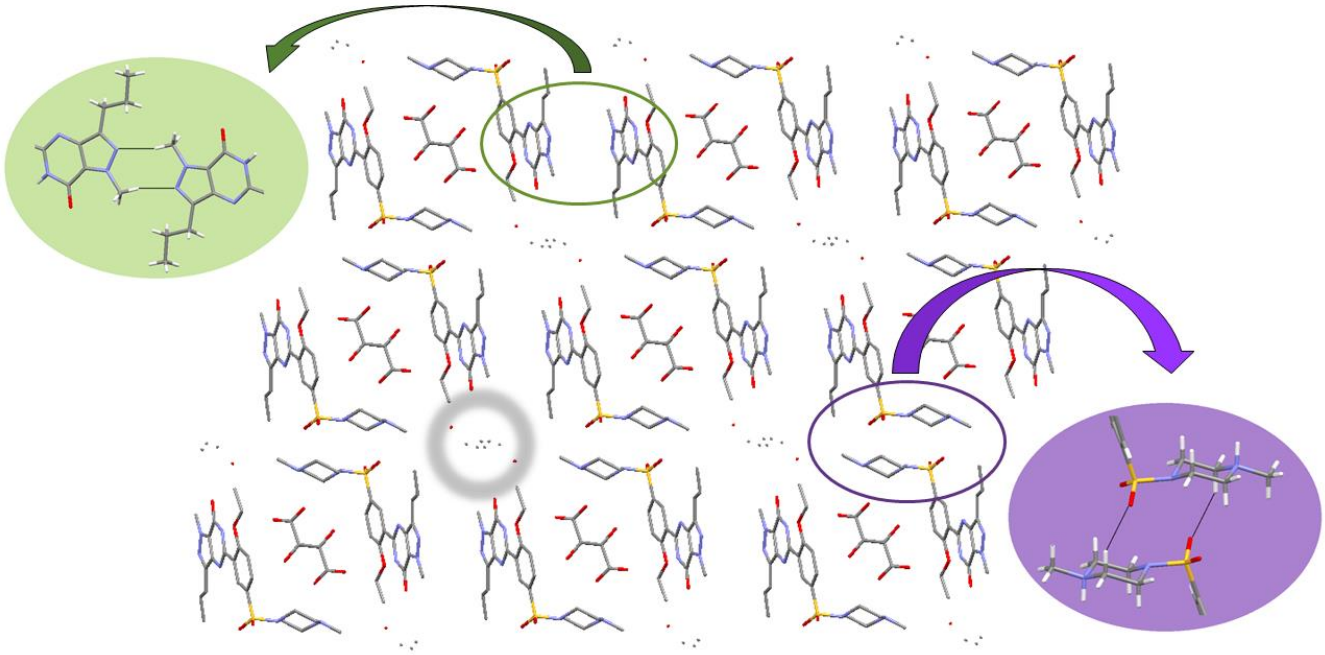

Figure 4: Crystal structure of tartaric acid salt of sildenafil (he tret isopropanol hemisolvate). The most relevant interactions have been highlighted. Channels filled by solvent molecules are highlighted with grey circles.

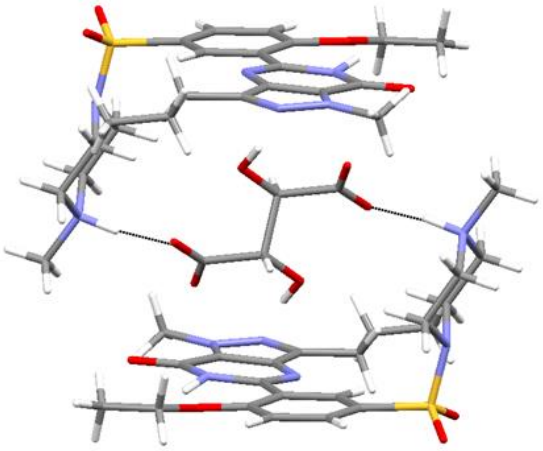

Figure 5: Sildenafil/tartrate cage in the crystal structure of tartaric acid salt of sildenafil (he tret isopropanol hemisolvate).

3.3.2 Hybrid 3-hydroxybenzoic acid salt/cocrystal monohydrate (SIL-3-HBA-IV)

The hybrid salt/cocrystal formed by 3-hydroxybenzoic acid and sildenafil crystallizes with one molecule of sildenafil cation, one molecule of the carboxylate, half molecule of the carboxylic acid and one molecule of water in the asymmetric unit. Chains of self-assembled sildenafil cations are formed through strong hydrogen bonds between the piperazinium ring and the carbonylic oxygen. As expected, strong charge-assisted hydrogen bonds are formed between the carboxylate anion and the piperazinium cation but one molecule of the non-ionized carboxylic acid interacts with the carboxylate anion via the phenol and carboxylic hydrogen in an alternate manner (fig. 9). Weak antiparallel dipole-dipole interactions between stacked pyrimidinone rings are established conferring extra stabilization to the crystal (fig 8).

In addition, one molecule of water is also present acting as a bridge between carboxylates (fig. 6). Non-ionized 3-hydroxybenzoic acid molecules are located in channels stablishing strong hydrogen bonds with other 3-hydroxybenzoate molecules (fig. 7).

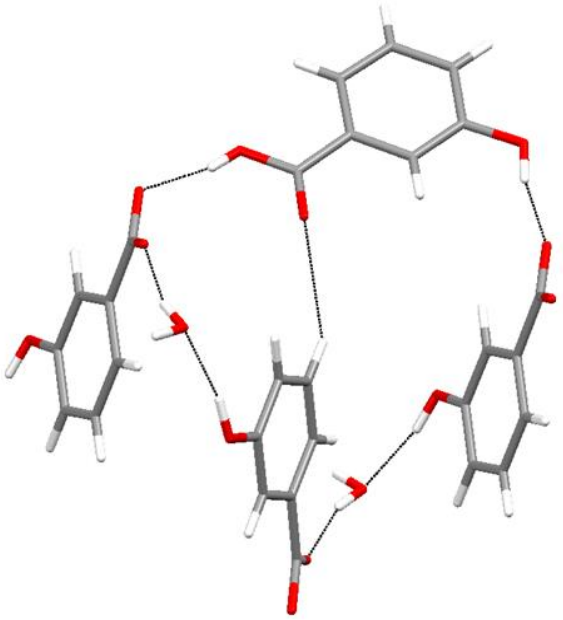

Figure 6: Chains of carboxylate/carboxylic acid molecules linked by molecules of water in the hybrid 3-hydroxybenzoic salt/cocrystal monohydrate

3.3.3 3-hydroxybenzoic acid salt THF hemisolvate sesquihydrate (SIL-3-HBA II)

The salt formed by 3-hydroxybenzoic acid and sildenafil crystallizes with one molecule of sildenafil cation, one molecule of the carboxylate, half disordered molecule of THF and 1.5 molecules of water in the asymmetric unit. In spite of the different degree of proton transfer this solid form is isostructural to the hybrid 3-hydroxybenzoic acid salt/cocrystal and the same interactions between sildenafil and 3-hydroxybenzoate molecules are stablished. Moreover, identical channels are formed but filled by disordered tetrahydrofurane and water molecules instead of molecules of 3-hydroxybenzoic acid. Only small differences between both structures are present like, for instance, centroid-centroid distances

measured between pyrimidinone rings and torsion angles of propyl groups (fig. 8).

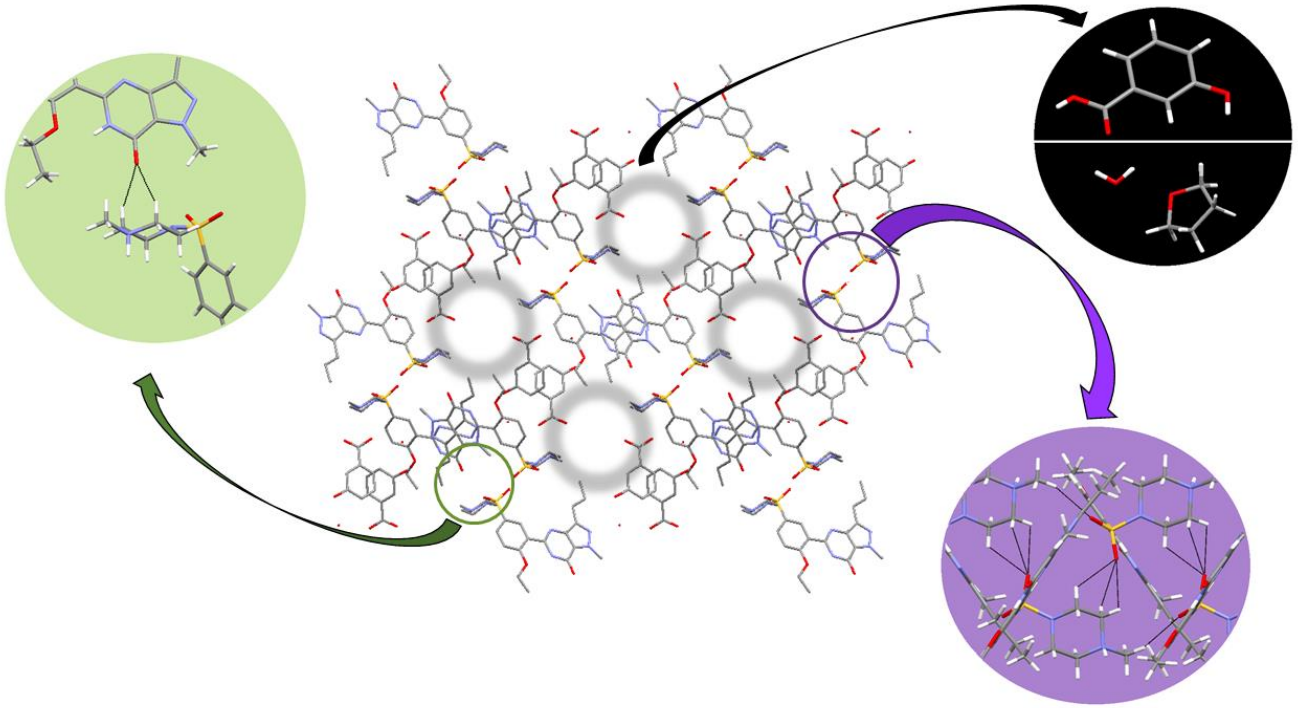

Figure 7: Representation of the crystal structures of 3-hydroxybenzoic acid salt and hybrid salt/cocrystal of sildenafil. The most relevant interactions have been highlighted and hydrogens have been partially omitted for clarity. Channels filled by THF and water molecules in the salt or 3-hydroxybenzoic molecules in the hybrid salt/cocrystal are highlighted with grey circles

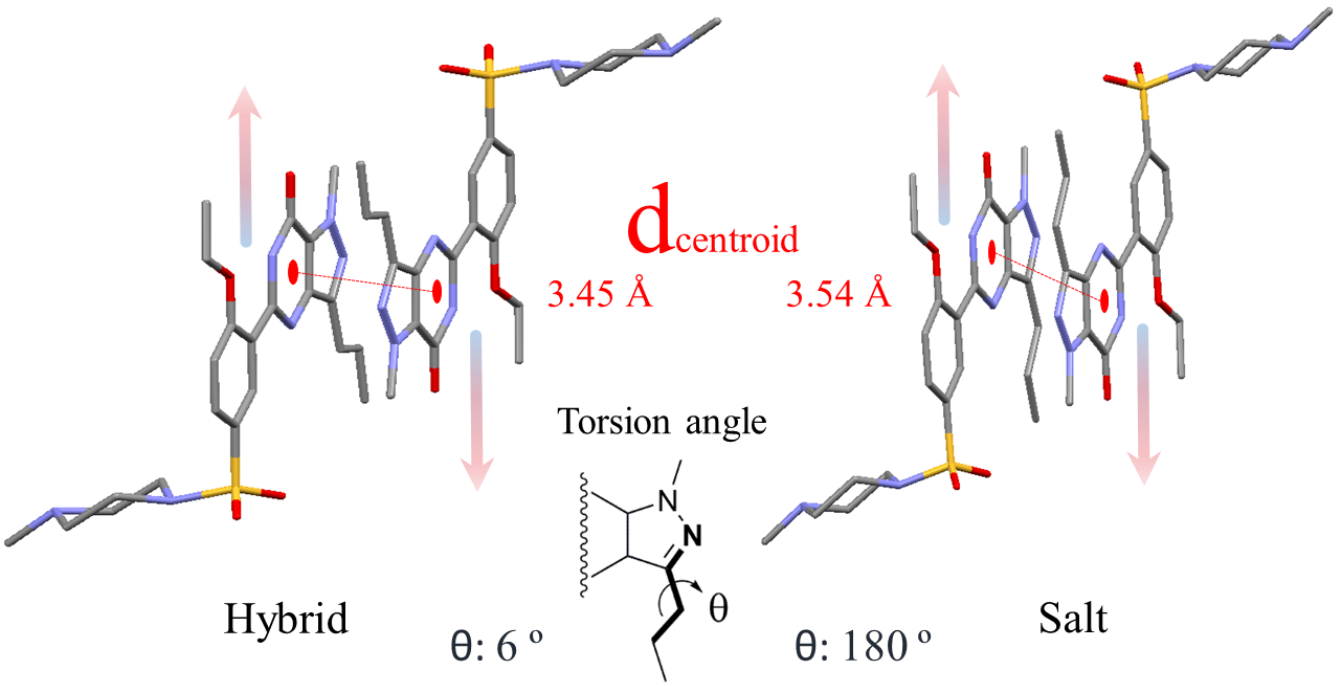

Figure 8: Antiparallel dipole-dipole interactions established between stacked pyrimidinone rings in the crystal structures of 3-hydroxybenzoic acid salt (right) and hybrid salt/cocrystal (left). Differences in centroid-centroid distances measured between pyrimidinone rings and torsion angles of propyl groups are shown for each structure.

3.3.4 Hybrid 3,4-dihydroxybenzoic acid salt/cocrystal monohydrate (SIL-3,4-DHBA IV)

The hybrid salt/cocrystal formed by 3,4-dihydroxybenzoic acid and sildenafil crystallizes with one molecule of sildenafil cations, one molecule of the carboxylate, half molecule of the carboxylic acid and one molecule of water in the asymmetric unit. This solid form is isostructural to the hybrid 3-hydroxybenzoic acid salt/cocrystal. The presence of an extra phenol group in the 3,4-dihydroxybenzoic acid only reinforces the same packing without disrupting any of the main observed interactions in the hybrid 3-hydroxybenzoic acid salt/cocrystal. Figure 9 shows chains of carboxylate molecules linked by water molecules in both structures.

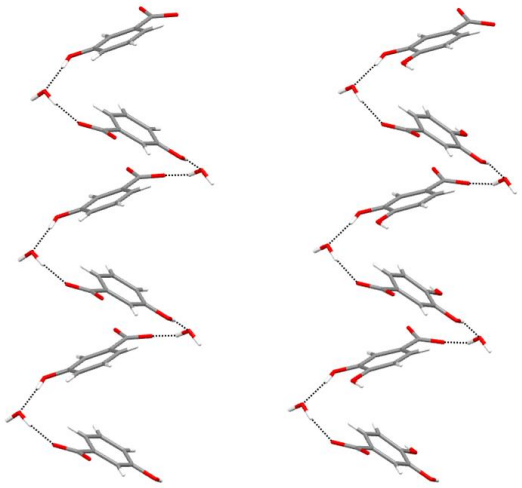

Figure 9: Chains of carboxylate molecules linked by molecules of water in the hybrid 3-hydroxybenzoic acid salt/cocrystal (left) and in the hybrid 3,4-dihydroxybenzoic acid salt/cocrystal (right).

3.3.5 Hybrid 3,4-dihydroxybenzoic acid salt/cocrystal acetonitrile disolvate (SIL-3,4-DHBA II)

The hybrid 3,4-dihydroxybenzoic acid salt/cocrystal acetonitrile disolvate crystallizes with one molecule of the sildenafil cation, one molecule of the carboxylate, one molecule of the carboxylic acid and two molecules of acetonitrile in the asymmetric unit. In a similar way that the tartaric acid salt,

instead of catemeric chains of sildenafil cations, self-assembled dimers are formed through charge-assisted hydrogen bonds (fig. 10).

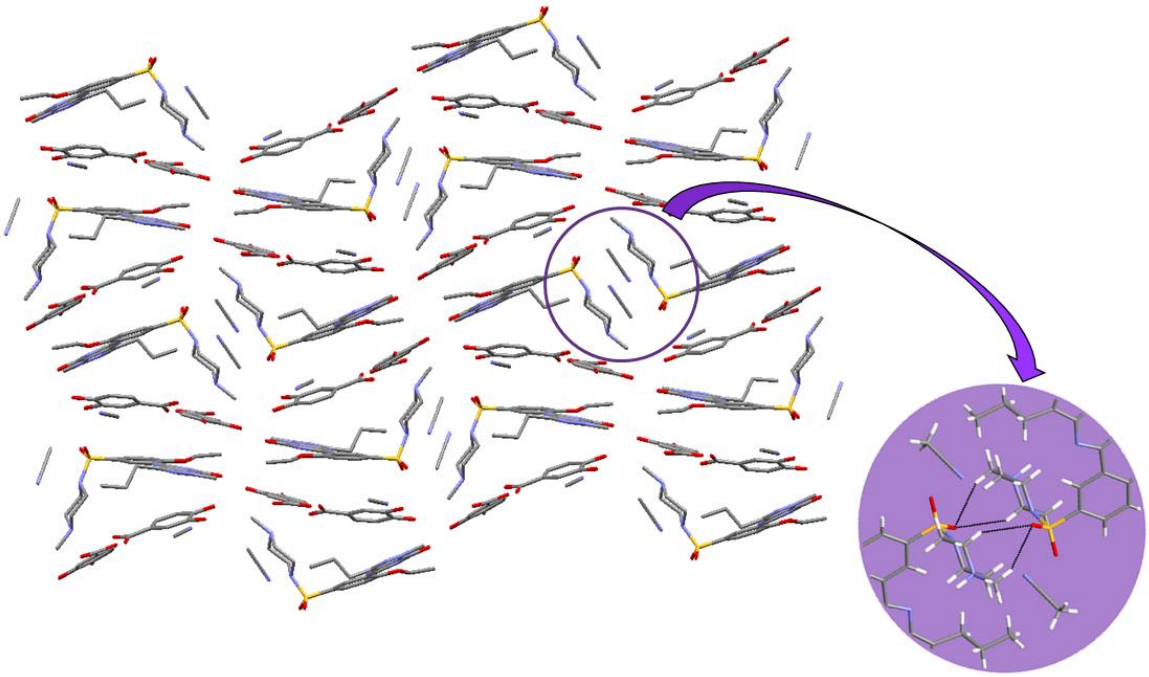

Figure 10. Crystal structure of 3,4-dihydroxybenzoic acid hybrid salt/cocrystal. Self-assembled dimers formed through charge-assisted hydrogen bonds are highlighted. Hydrogens have been partially omitted for clarity.

However, the antiparallel dipole-dipole interactions between stacked pyrimidinone rings are not observed in this form. This is the only structure of this family of hybrid salts/cocrystals where water is not present and this produces a different architecture of the coformer self-assembling which consists of layers of alternate carboxylic/carboxylate interactions (fig. 11).

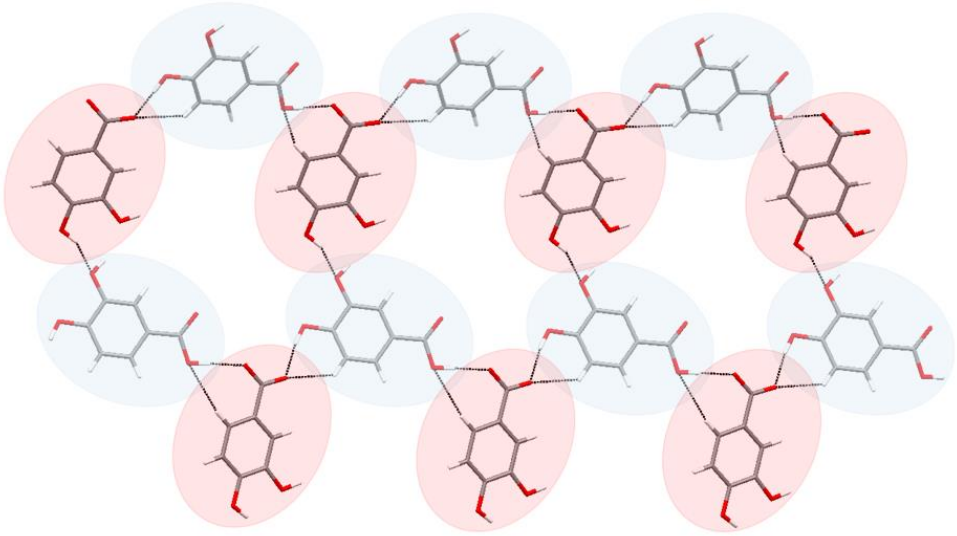

Figure 11: Layers of alternate carboxylic (blue)/carboxylate (red) interactions.

3.4 Dissolution study

The dissolution studies were carried out at pH 1.2, pH 6.5 and FaSSIF (pH 6.5) which represent the average pH values of the fast state stomach and intestine respectively. SIL has pH dependent solubility which decreases with increase in pH. One of the major challenges in the dissolution study of multicomponent entities is continuous change in the solution composition due to precipitation of either of the component over dissolution testing period. The solubility data generated may be erroneous due to limitations of the analytical method for example estimations carried out by UV spectrophotometry are subject to the overlap in the absorption spectra of the two components. We have used HPLC method to quantify amount of SIL dissolved, hence we see some difference in reported dissolutions compared to the previous SIL salt dissolution data reported *(P Sanphui, S Tothadi, S Ganguly and G R Desiraju, 2013, Mol Pharmaceutics, 10, 4687-4697)*.

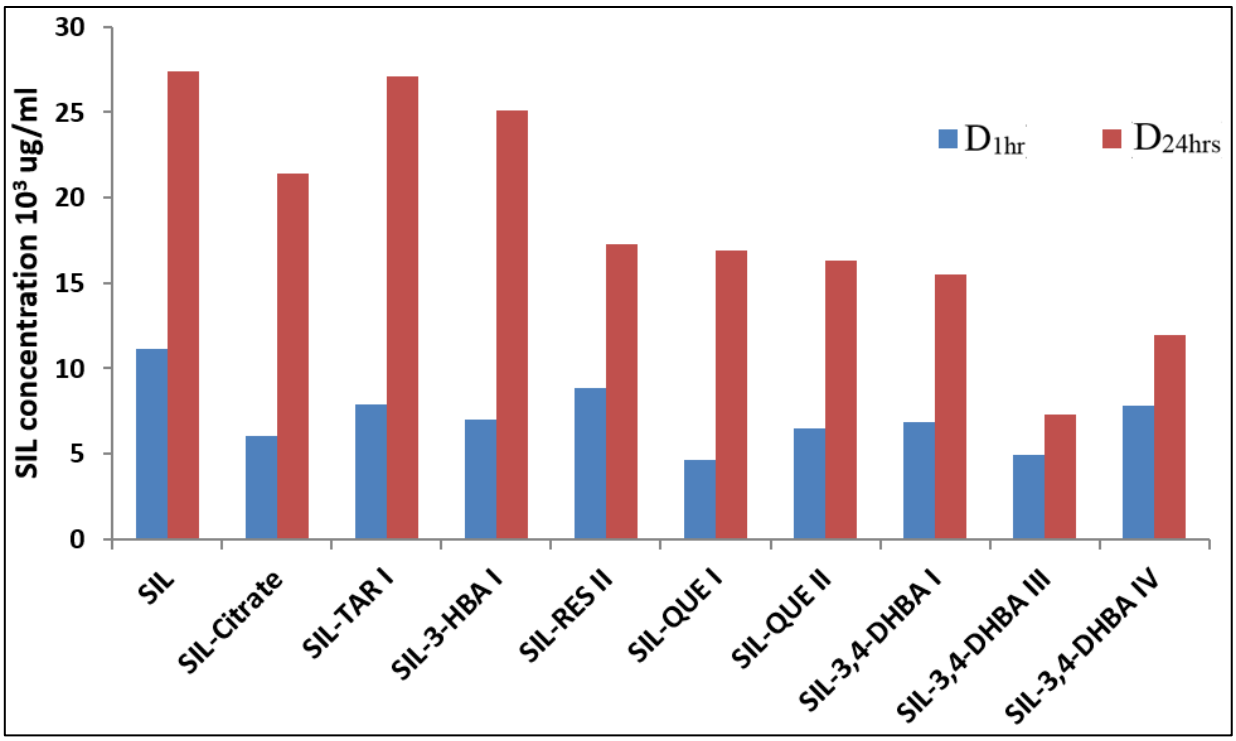

Figure 12: Comparative solubility of SIL salts, cocrystals and hybrid salt-cocrystals in 0. 1N HCl (pH 1.2)

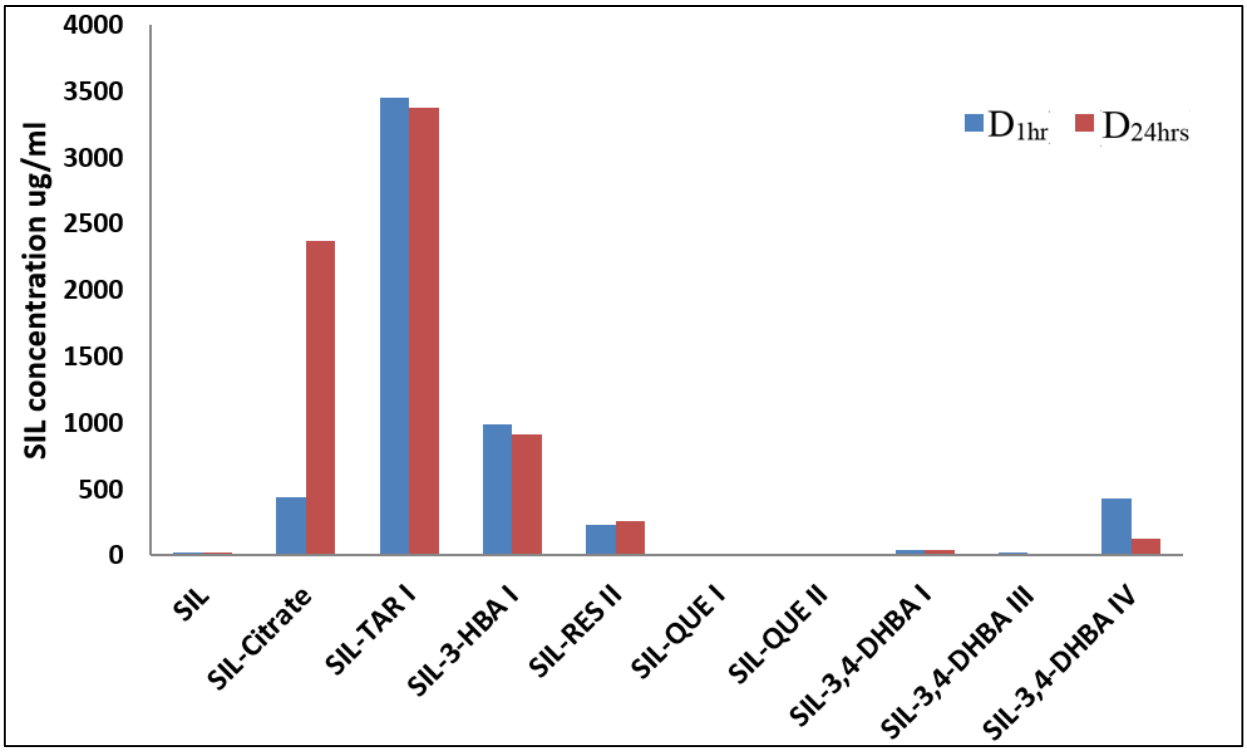

Figure 13: Comparative solubility of SIL salts, cocrystals and hybrid salt-cocrystals in phosphate buffer pH 6.5

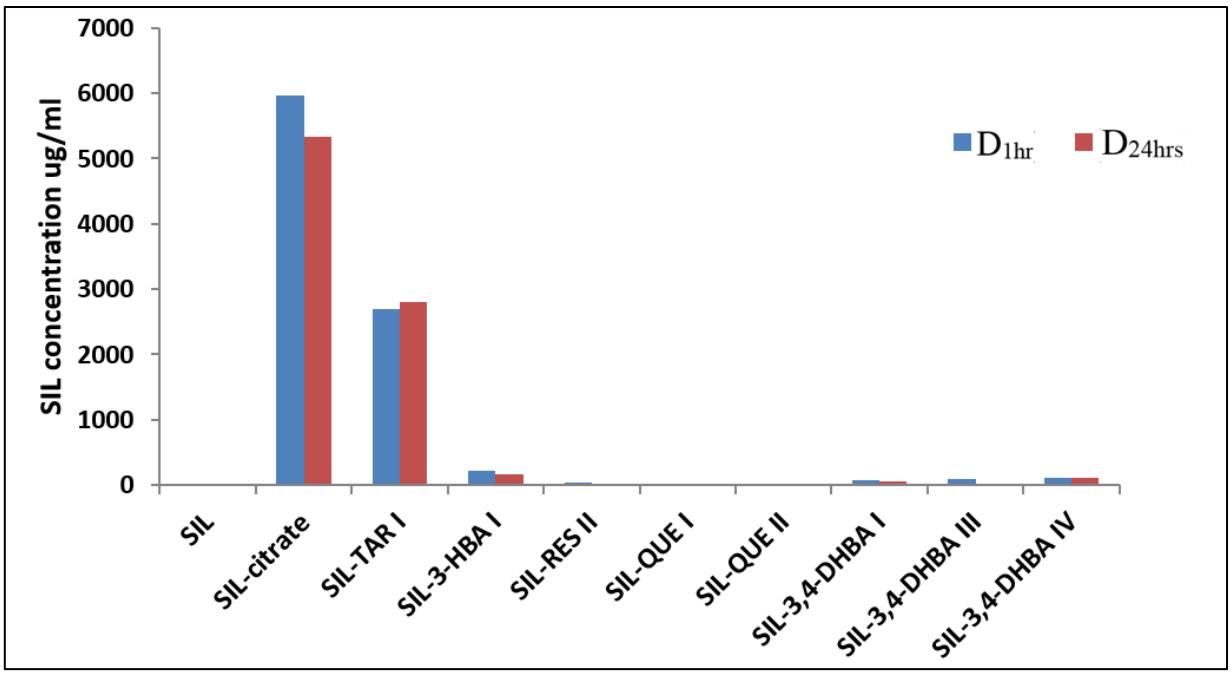

Figure 14: Comparative solubility of SIL salts, cocrystals and hybrid salt-cocrystals in FaSSIF

At pH 1.2 the amount dissolved from SIL salts was significantly higher than the cocrystals and HSC form. The HSCs except SIL-3,4-DHBA I showed poor dissolution performance compared to cocrystals. SIL-TAR I showed significantly high dissolution rate compared to SIL-CIT a commercially used salt of SIL. The D_{1hr} and D_{24hrs} values for SIL-TAR I was significantly higher than SIL-CIT. At pH 1.2 in the salt category SIL-TAR > SIL-3-HBA I > SIL-CIT. Though D_{1hr} for SIL-RES II > SIL-QUE I and SIL – QUE II. It is interesting to note that the amount dissolved at pH 6.5 though was at least 10 times lower than the amount dissolved at pH 1.2. But amount of SIL dissolved was significantly higher than cocrystals and HSCs. Most of the cocrystals and HSCs did not provide any release of SIL at pH 6.5 or even in FaSSIF , which contains additive like lecithin is included in the dissolution media. The dissolution study demonstrates potential of SIL-TAR as a better alternative to SIL – CIT.

4. CONCLUSIONS

In summary, we have revisited the multicomponent solid form landscape of sildenafil by conducting a combined virtual and experimental screening. 23 new solid forms have been discovered and characterized and the intrinsic dissolution rate have been measured for some of the solid forms. However, none of them showed a better profile than the citrate salt. The analysis of the five crystal

structures solved by SXRD showed a variety of salts and hybrid salt/cocrystals with different hydrogen bond architectures and presence of solvent channels. This study extends the knowledge about the solid state of this important drug compound, contributes with new cases to the body of data of unexpected stoichiometric hybrid salt/cocrystals and it is a new example of successful application of combined virtual/experimental methodologies for the discovery of new solid forms.

5. SUPPORTING INFORMATION

Synthesis of different crystal forms. Crystal data and structure refinement. Cocrystal Screening experiments. Characterization of the solids: DSC and TGA thermograms, PXRD diffractograms, ^{1}H-NMR spectra of new crystal forms. This material is available free of charge via the Internet at http://pubs.acs.org

6. REFERENCES

1 Blagden, N.; de Matas, M.; Gavan, P.T.; York, P. Crystal engineering of active pharmaceutical ingredients to improve solubility and dissolution rates *Adv Drug Deliv Rev* **2007**, *59*, 617–630.

2 Almarsson, O.; Zaworotko, M. J. Crystal engineering of the composition of pharmaceutical phases. Do pharmaceutical co-crystals represent a new path to improved medicines? *Chem. Commun*. **2004**, 1889-1896.

3 Bolla, G.; Sanphui, P.; Nangia, A. Solubility Advantage of Tenoxicam Phenolic Cocrystals Compared to Salts *Cryst. Growth Des.* **2013**, *13*, 1988-2003.

4 Good, D.J.; Rodriguez-Hornedo, N. Solubility Advantage of Pharmaceutical Cocrystals *Cryst. Growth Des.* **2009**, *9*, 2252-2264

5 Liu, X.; Lu, M.; Guo, Z.; Huang, L.; Feng, X.; Wu, C. Improving the Chemical Stability of Amorphous Solid Dispersion with Cocrystal Technique by Hot Melt Extrusion *Pharm Res.* **2012**, *29*, 806-817.

6 Food and Drug Administration *Regulatory Classification of Pharmaceutical Co-Crystals Guidance for Industry*. **2018**.

7 Rajesh Thipparaboina, R.; Kumar, D.; Mittapalli, S.; Balasubramanian, S.; Nangia, A.; Shastri, N.R. Ionic, Neutral, and Hybrid Acid-Base Crystalline Adducts of Lamotrigine with Improved

Pharmaceutical Performance *Cryst. Growth Des.* **2015**, *15 (12)*, 5816–5826.

8 Barnett, C. F.; Machado, R. F. Sildenafil in the treatment of pulmonary hypertension. *Vasc Health Risk Manag*. **2006**, *2(4)*, 411–422.

9 Galiè, N.; Hoeper, M.M.; Humbert, M.; Torbicki, A.; Vachiery, J. L.; Barbera, J. A.; Beghetti, M.; Corris, P.; Gaine, S.; Gibbs, J. S.; Gomez-Sanchez, M. A.; Jondeau, G.; Klepetko, W.; Opitz, C.; Peacock, A.; Rubin, L.; Zellweger, M.; Simonneau, G.; ESC Committee for Practice Guidelines (CPG) Guidelines for the diagnosis and treatment of pulmonary hypertension: The Task Force for the Diagnosis and Treatment of Pulmonary Hypertension of the European Society of Cardiology (ESC) and the European Respiratory Society (ERS), endorsed by the International Society of Heart and Lung Transplantation (ISHLT). *Eur Heart J.* **2009**, *30(20)*, 2493-2537.

10 Jung S.Y.; Seo Y.G.; Kim G.K.; Woo J.S.,; Yong C.S.; Choi H.G. Comparison of the solubility and pharmacokinetics of sildenafil salts. *Arch Pharm Res*. **2011**, *34(3)*, 451-454.

11 Sanphui, P.; Tothadi, S.; Ganguly, S.; Desiraju, G. R. Salt and Cocrystals of Sildenafil with Dicarboxylic Acids: Solubility and Pharmacokinetic Advantage of the Glutarate Salt *Mol. Pharmaceutics* **2013**, *10*, 4687-4697.

12 Stepanovs, D.; Mishnev, A. Molecular and Crystal Structure of Sildenafil Base. *Z. Naturforsch.* **2012**, *67b*, 491–494. CSD code QEGTUT.

13 Barbas, R.; Font-Bardia, M.; Prohens, R. Polymorphism of Sildenafil: A New Metastable Desolvate *Cryst. Growth Des.* **2018**, *18*, 3740−3746.

14 Barbas, R.; Prohens, R.; Font-Bardia, M.; Bauzá, A.; Frontera, A. Hydrogen bonding versus π-interactions: their keycompetition in sildenafil solvates DOI: 10.1039/c8ce00567b.

15 Cresset torchV10lite. http://www.cresset-group.com/products/torch/torchlite/.

16 Frisch, M. J.; Trucks, G. W.; Schlegel, H. B.; Scuseria, G. E.;Robb, M. A.; Cheeseman, J. R.; Scalmani, G.; Barone, V.; Mennucci, B.; Petersson, G. A.; Nakatsuji, H.; Caricato, M.; Li, X.; Hratchian, H. P.; Izmaylov, A. F.; Bloino, J.; Zheng, G.; Sonnenberg, J. L.; Hada, M.; Ehara, M.; Toyota, K.; Fukuda, R.; Hasegawa, J.; Ishida, M.; Nakajima, T.; Honda, Y.; Kitao, O.; Nakai, H.; Vreven, T.; Montgomery, J. A., Jr.; Peralta, J. E.; Ogliaro, F.; Bearpark, M.; Heyd, J. J.; Brothers, E.; Kudin, K. N.; Staroverov, V. N.; Kobayashi, R.; Normand, J.; Raghavachari, K.; Rendell, A.; Burant, J. C.; Iyengar, S. S.; Tomasi, J.; Cossi, M.; Rega, N.; Millam, N. J.; Klene, M.; Knox, J. E.; Cross, J. B.; Bakken, V.; Adamo, C.; Jaramillo, J.; Gomperts, R.; Stratmann, R. E.; Yazyev, O.; Austin, A. J.; Cammi, R.; Pomelli, C.; Ochterski, J. W.; Martin, R. L.; Morokuma, K.; Zakrzewski, V. G.; Voth, G. A.; Salvador, P.; Dannenberg, J. J.; Dapprich, S.; Daniels, A.D.; Farkas, Ö.; Foresman, J. B.; Ortiz, J. V.; Cioslowski, J.; Fox, D. J. Gaussian 09; Gaussian, Inc.: Wallingford, CT, 2009.

17 Calero, C. S.; Farwer, J.; Gardiner, E. J.; Hunter, C. A.; Mackey, M.; Scuderi, S.; Thompson, S.;

Vinter, J. G. Footprinting molecular electrostatic potential surfaces for calculation of solvation energies *Phys. Chem. Chem. Phys*. **2013**, *15*, 18262−18273.

18 SADABS Bruker AXS; Madison, Wisconsin, USA, **2004**; SAINT, Software Users Guide, Version 6.0; Bruker Analytical X–ray Systems, Madison, WI, **1999**. Sheldrick, G. M. SADABS v2.03: Area–Detector Absorption Correction. University of Göttingen, Germany, **1999**; Saint Version 7.60A (Bruker AXS 2008); SADABS V. 2008–1 (**2008**).

19 Sheldrick, G. M. A short history of SHELX. *Acta Cryst*. **2008**, *A64*, 112–122.

20 Boultif, A.; Louër, D. Indexing of powder diffraction patterns for low-symmetry lattices by the successive dichotomy method. *J. Appl. Crystallogr*. **1991**, *24*, 987–993.

21 Grecu, T.; Hunter, C. A.; McCabe, J.; Gardiner, E. J. Validation of a Computational Cocrystal Prediction Tool: Comparison of Virtual and Experimental Cocrystal Screening Results *Cryst. Growth Des*. **2014**, *14*, 165−171.

22 Hunter, C. A., A surface site interaction model for the properties of liquids at equilibrium *Chem. Sci.* **2013**, *4*, 1687-1700.

23 Hunter, C. A. Quantifying Intermolecular Interactions: Guidelines for the Molecular Recognition Toolbox *Angew. Chem., Int. Ed*. **2004**, *43*, 5310−5324.

Byard, S.; Abraham, A.; Boulton, P. J. T.; Harris, R. K.; Hodgkinson, P. A multi-technique approach to the study of structural stability and desolvation of two unusual channel hydrate solvates of finasteride. *J. Pharm. Sci*., **2012**, *101*, 176-186.

24 Etter, M. C. Hydrogen Bonds as Design Elements in Organic Chemistry *J. Phys. Chem*. **1991**, *95*, 4601−4610.

25 (b) For an analysis that considers only pairing of the most polar sites, see the following: Aakeroy, C. B.; Desper, J.; Smith, M. M. Constructing, deconstructing, and reconstructing ternary supermolecules *Chem. Commun*. **2007**, *0*, 3936−3938.

26 International Union of Pure and Applied Chemistry (IUPAC); Stahl, P. H.; Wermuth, C. G. Handbook of pharmaceutical salts: properties, selection, and use Weinheim; New York: VHCA: Wiley-VCH, **2002**.

27 Childs, S. L.; Stahly, G. P.; Park, A. The Salt-Cocrystal Continuum: The Influence of Crystal Structure on Ionization State. *Mol. Pharmaceutics* **2007**, *4*, 323−338

28 Cruz-Cabeza, A. J. Acid–base crystalline complexes and the pKa rule *CrystEngComm* **2012**, *14*, 6362-6365.

29 Gobry, V.; Bouchard, G.; Carrupt, P.A.; Testa, B.; Girault, H. H. Physicochemical Characterization of Sildenafil: Ionization, Lipophilicity Behavior, and Ionic-Partition Diagram Studied

by Two-Phase Titration and Electrochemistry *Helvetica Chimica Acta* **2000**, *83*, 1465-1474.

30 pKa value: Musialik, M.; Kuzmicz, R.; Pawłowski, T. S. Litwinienko, G. Acidity of Hydroxyl Groups: An Overlooked Influence on Antiradical Properties of Flavonoids *J. Org. Chem*. **2009**, *74(7)*, 2699-2709.

31 pKa values: FooDB Database. http://foodb.ca/

32 pKa values: Internet Bond-energy Databank (iBonD). http://ibond.chem.tsinghua.edu.cn

33 pKa values: Tao, L.; Han, J.; Tao, F.G. Correlations and Predictions of Carboxylic Acid pKa Values Using Intermolecular Structure and Properties of Hydrogen-Bonded Complexes *J. Phys. Chem. A*, **2008**, *112 (4)*, 775–782.

34 Jacobs, A.; Amombo Noa, F.M. Hybrid Salt-Cocrystal Solvate: *p*-Coumaric Acid and Quinine System *J. Chem Crystallogr*. **2014**, *44*, 57-62.

35 Mahieux, J.; Gonella, S.; Sanselmea, M.; Coquerel, G. Crystal structure of a hybrid salt–cocrystal and its resolution by preferential crystallization: ((±)trans-N,N′-dibenzyldiaminocyclohexane)(2,3-dichlorophenylacetic acid)$_4$ *CrystEngComm*, **2012**,*14*, 103-111.

36 Aakeröy, C. B.; Fasulo, M.E.; Desper, J. Cocrystal or Salt: Does It Really Matter? *Mol. Pharmaceutics*, **2007**, *4(3)*, 317–322.

37 Methanol, ethanol, IPA, butanol, 1-propanediaol, glycerol, ethylene glycol, 2-methoxyethanol, 1-propanol, 1-pentanol, 1-octanol, 2,2,2-trifluoroethanol, benzyl alcohol, ACN, propionitrile, MEK, acetone, MiBK, water, DMF, DMSO, pentane, heptane, cyclohexane, hexane, methylcyclohexane, toluene, xylene, mesitylene, anisole, 2-nitrotoluene, nitrobenzene, AcOEt, isopropyl acetate, diethylether, THF, 1-methyl-2-pyrrolidone, dimethyl ethylene glycol, diisopropyl ether, dioxane, iodomethane, dichloromethane, 1,2-dichlorothane, chloroform, 1,1,1-trichloroethane, 1,1,2-trichloroethane, formic acid, acetic acid, trifluoroacetic acid, propanoic acid, NH3 (32%) in water, diethylamine, trimethylamine and pyridine.

38 Issa, M.G.; Ferraz, H. G. Dissolution Technologies Intrinsic Dissolution as a Tool for Evaluating Drug Solubility in Accordance with the Biopharmaceutics Classification System *Dissolution Technol.* **2011**, *18*, 6-13.

For Table of Contents Use Only

Combined Virtual/Experimental Multicomponent Solid Forms Screening of Sildenafil: New Salts, Cocrystals and Hybrid Salt-Cocrystals

Rafael Barbas,[†] *Mercè Font-Bardia,*[§] *Anant Paradkar,*[∥] *Christopher A. Hunter*[‡] *and Rafel Prohens**[†]

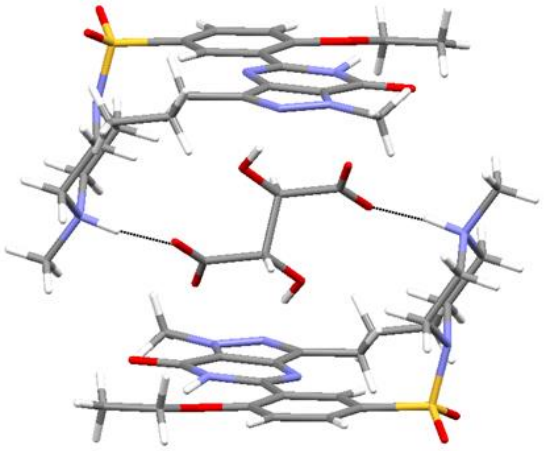

SYNOPSIS TOC. New multicomponent solid forms of Sildenafil have been discovered by means of a combined virtual/experimental cocrystal screening. Coformer selection of candidates was conducted based on an *in silico* screening method from a database of more than 2000 organic compounds and the intensive experimental screen produced 24 new solid forms. Since the 12 coformers chosen have a combination of phenol and carboxylic acid groups a variety of cocrystals, salts and hybrid salt/cocrystals were discovered and characterized.